Parameter selection with the Hotelling observer in linear iterative image reconstruction for breast tomosynthesis

Sean D. Rose, Jacob Roth, Cole Zimmerman, Ingrid Reiser, Emil Y. Sidky, et al.

Sean D. Rose, Jacob Roth, Cole Zimmerman, Ingrid Reiser, Emil Y. Sidky, Xiaochuan Pan, "Parameter selection with the Hotelling observer in linear iterative image reconstruction for breast tomosynthesis," Proc. SPIE 10577, Medical Imaging 2018: Image Perception, Observer Performance, and Technology Assessment, 105770P (7 March 2018); doi: 10.1117/12.2293805

SPIE.

Event: SPIE Medical Imaging, 2018, Houston, Texas, United States

Parameter Selection with the Hotelling Observer in Linear Iterative Image Reconstruction for Breast Tomosynthesis

Sean D. Rose, Jacob Roth, Cole Zimmerman, Ingrid Reiser, Emil Y. Sidky, and Xiaochuan Pan

The University of Chicago Dept. of Radiology MC-2026, 5841 S. Maryland Avenue, Chicago IL, 60637

ABSTRACT

In this work we investigate an efficient implementation of a region-of-interest (ROI) based Hotelling observer (HO) in the context of parameter optimization for detection of a rod signal at two orientations in linear iterative image reconstruction for DBT. Our preliminary results suggest that ROI-HO performance trends may be efficiently estimated by modeling only the 2D plane perpendicular to the detector and containing the X-ray source trajectory. In addition, the ROI-HO is seen to exhibit orientation dependent trends in detectability as a function of the regularization strength employed in reconstruction. To further investigate the ROI-HO performance in larger 3D system models, we present and validate an iterative methodology for calculating the ROI-HO. Lastly, we present a real data study investigating the correspondence between ROI-HO performance trends and signal conspicuity. Conspicuity of signals in real data reconstructions is seen to track well with trends in ROI-HO detectability. In particular, we observe orientation dependent conspicuity matching the orientation dependent detectability of the ROI-HO.

Keywords: digital breast tomosynthesis, model observers, iterative image reconstruction

1. PURPOSE

Implementation of iterative image reconstruction for digital breast tomosynthesis (DBT) involves a number of parameter choices, such as voxel size, voxel aspect ratio, projection model, and regularization strength. The detection of subtle features in DBT reconstructions, such as small microcalcifications or fine spiculations, can potentially be affected by each of these choices. The parameter dependence of these algorithms needs to be characterized for every task and system design under consideration, and efficiently computable task-based simulation metrics are required for this purpose.

While much effort has been devoted to the optimization of system parameters in DBT,[1] the work has predominately focused on two clinically relevant detection tasks: (1) the detection of small, high-contrast microcalcifications and (2) the detection of large, low contrast lesions. These tasks are typically modeled with rotationally symmetric signals of different size and contrast. There are, however, a number of clinically relevant tasks for which the signal of interest is asymmetric. For example, the detection of spiculated lesions, Cooper's ligaments, and blood vessels all involve rotationally invariant signals. These tasks involve the detection of thin, fiber-like signals that can exhibit orientation-dependent conspicuity in DBT.[2]

The purpose of this work is the application and investigation of an efficient implementation of a region-of-interest (ROI) based Hotelling observer (HO), developed in our previous work,[3] to the detection of a rod signal in linear iterative image reconstruction for DBT. The implementation avoids the use of noise realizations as we are interested in sweeping out the multidimensional parameter spaces involved in iterative image reconstruction without performing excessively large numbers of reconstructions. The implementation employs a 2D system model for efficient evaluation of the ROI-HO. In recent work we validated this implementation via comparison to calculations of the ROI-HO employing a 3D system model for a small, high-contrast speck signal.[4] Here we continue to investigate the 2D system model, but for detection of an asymmetric rod signal at two orientations.

We first investigate the use of a 2D system model for DBT in evaluating the ROI-HO via a simulation study investigating the regularization strength dependence of rod detection with Tikhonov regularized least squares reconstruction. The results of the 2D calculation are compared to evaluation of the ROI-HO with a 3D system model. We then present and validate an iterative methodology for calculation of the ROI-HO that should

Medical Imaging 2018: Image Perception, Observer Performance, and Technology Assessment, edited by Robert M. Nishikawa, Frank W. Samuelson, Proc. of SPIE Vol. 10577, 105770P
 · doi: 10.1117/12.2293805

allow for calculation of the ROI-HO with larger 3D system models and tasks of larger spatial extent. Lastly, we investigate correspondence between ROI-HO efficiency trends and conspicuity of a rod signal in real data reconstructions using the ACR digital mammography accreditation phantom.

2. METHODS

2.1 Reconstruction Optimization Problem

We confine our focus to Tikhonov regularized least square (PLS) reconstruction optimization problems of the form

$$\min_x \|Ax - y\|^2 + \lambda\|x\|^2$$

where $x \in \Re^n$ is an image vector, $A \in \Re^{m\times n}$ is a linear forward model for X-ray projection, and $y \in \Re^m$ is the post-log (sinogram) data. As the problem is quadratic in x, the solution can be written as a linear function of the data

$$x^* = Ry$$
$$R = (A^TA + \lambda I)^{-1}A^T$$

where the matrix $R \in \Re^{n\times m}$ will be referred to as the reconstruction matrix.

2.2 ROI-HO

We consider calculating the HO for detection of a signal within an ROI defined by a mask operation $M \in \Re^{p\times n}$. The operator M takes an input image and returns the portion of the image within the ROI. Denoting the signal absent case by H_0 and the signal present case by H_1, we consider the following model for each case

$$H_0 : x_{\text{ROI}} = MR(b_y + n_y)$$
$$H_1 : x_{\text{ROI}} = MR(b_y + n_y + s_y)$$

where b_y, n_y, and s_y denote the background, quantum noise, and signal in the post-log data domain.

The HO template for this detection task is defined implicitly via the equation[5]

$$K_{\text{ROI}}w = s_{\text{ROI}}$$

where K_{ROI} is the average of the signal absent and signal present covariance matrices of x_{ROI}, w is the HO template, and s_{ROI} is the average reconstructed and masked signal. Denoting the average data domain covariance of the signal absent and present cases by K_y, we can rewrite the previous equation as

$$MRK_yR^TM^Tw = MRs_y \tag{1}$$

where we have propagated the data domain covariance through the mask and reconstruction operations.

The figure of merit we report in our studies is the efficiency ϵ, given by

$$\epsilon = \frac{\text{SNR}^2_{\text{ROI}}}{\text{SNR}^2_y}$$

where

$$\text{SNR}^2_{\text{ROI}} = w^Ts_{\text{ROI}}$$

is the signal-to-noise-ratio (SNR) of the ROI-HO in the masked reconstruction and

$$\text{SNR}^2_y = s_y^T(K_y^{-1}s_y)$$

is the SNR of the HO in the post-log data domain. The efficiency characterizes the preservation of signal detectability through the process of reconstruction and masking and can be at most 1.0.

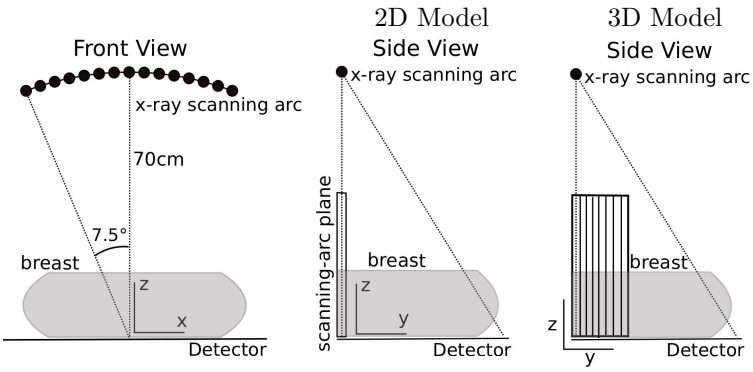

Figure 1. Schematic illustrating geometries used for 2D and 3D simulation studies.

2.3 2D System Model for Calculating the ROI-HO

To efficiently calculate the ROI-HO, the DBT system model is restricted to a 2D plane perpendicular to the detector and containing the X-ray source trajectory, which we refer to as the scanning-arc plane (see Figure 1). The idea of using the scanning-arc plane is that the principle imaging properties of DBT can be captured in this plane. The mask operator M was defined to restrict the observer to a 1.26 cm region of a single row of the reconstructed image containing the true volume of the signal. The resulting task is analogous to the case of signal detection from a single in-plane (x-y) slice in 3D DBT image reconstruction. Evaluation of the ROI-HO is done via direct methods since the reconstruction operator can be stored for a 2D system.

2.4 2D-3D Comparison Study

The first study investigates how well the ROI-HO evaluated with the 2D system model approximates the ROI-HO calculated using a 3D system model. We investigated this question in the context of characterizing the detection of a rod signal of 0.35 mm diameter and 1.1 mm length in a uniform background as a function of regularization strength with PLS reconstruction. The length of the rod was chosen so that, when oriented perpendicular to the scanning-arc plane, the rod was fully contained in the small 3D image volume employed in the 3D calculation of the ROI-HO. The 3D image volume included the 10 closet planes to the scanning arc plane. This is illustrated in the right panel of figure 1.

Analogous to the 2D implementation of the ROI-HO, the mask operator M for the 3D ROI-HO restricted the observer to a 1.26 cm $\times$ 0.14 cm ROI (10 slices being 0.14 cm in width) of a single in-plane slice containing the true signal. The 3D system was small enough the ROI-HO efficiencies could still be calculated using direct methods. Efficiencies for the rod signal were calculated at two orientations, one in which the rod was oriented at 0° with respect to the x axis (see Figure 1) and one in which it was oriented at 90°.

2.5 Iterative Method for Calculating the HO

The problem of finding the ROI-HO template in equation 1 can be equivalently posed as an equality constrained least squares problem (LSE)

$$\begin{aligned} &\min_u \|K_y^{\frac{1}{2}} A u - K_y^{-\frac{1}{2}} s_y\|^2 \\ \text{such that} \quad &(I - M^T M)(A^T A + \lambda I)u = 0 \end{aligned} \tag{2}$$

where $u \in \Re^n$ and the HO template is found from the solution u^* of the above via the equation

$$w^* = M(A^T A + \lambda I)u^* \tag{3}$$

Equation 2 can be rewritten as a symmetric indefinite linear system[6] and solved using standard linear methods, such as MINRES.[7] The key advantage to this formulation over that in equation 1 is that it does not require explicit calculation of the reconstruction matrix R and so can be extended to system models in which the dimensionality of A is large (i.e. 3D system geometries).

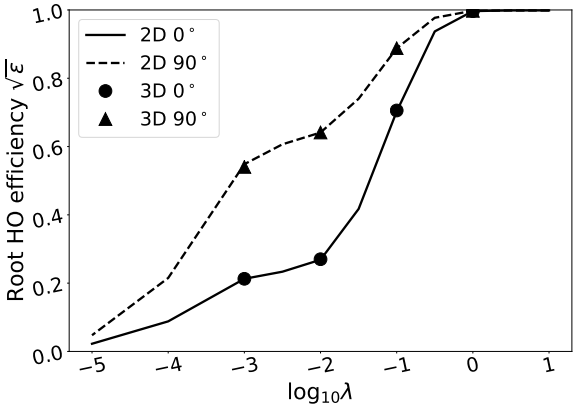

Figure 2. Comparison of ROI-HO efficiencies calculated using the 2D and 3D system models for a rod signal of 0.35 mm diameter and 1.1 mm length. Results are shown for both 0° and 90° orientations with respect to the x axis.

2.6 Verification Study

We performed a simulation study to verify that calculating the HO using equation 2 yields the same results as calculating it directly from equation 1. For this study we refer to equation 1 as the direct method and 2 as the LSE method. Using the 2D system model, the ROI-HO template was calculated at different regularization strengths λ for PLS using the direct and LSE methods and the efficiency was plotted as a function of regularization strength for both methods. For this study, a rod signal of 0.75 mm diameter and 10.0 mm length, modeling the second thickest fiber in the ACR digital mammography accreditation phantom, was investigated. The rod was oriented at 0° with respect to the x axis. We also performed the study for a rod signal of 0.61 diameter and 10.0 mm length oriented at 90°, modelling the third thickest rod in the phantom.

2.7 Real Data

To investigate whether the efficiency trends observed in simulation were reflective of conspicuity trends observable with real data, we performed a real data study using data acquired from an ACR mammography accreditation phantom with a Hologic Selenia Dimensions tomosynthesis system. The phantom was oriented so the second thickest fiber lay parallel to the x axis, matching the model for the fiber in the verification study above. PLS reconstructions were performed using the method of conjugate gradients and run to numerical convergence.

3. RESULTS

The ROI-HO efficiencies calculated using the 2D and 3D system models are shown in figure 2. The efficiencies for the 2D and 3D system models match closely over the range of regularization strengths investigated. The efficiency curves increase with increasing regularization strength from 0.0 up to a point of saturation at which the maximum possible efficiency of 1.0 is nearly achieved, though the transition from low to high efficiency appears to be orientation dependent, with the 90° signal exhibiting higher efficiencies at lower regularization strengths.

The ROI-HO efficiencies calculated by the LSE method are shown with curves calculated via the direct method in figure 3. There is good agreement between the two methods for regularization strengths $\log_{10}\lambda > -1.5$. At lower regularization strengths the convergence rate of MINRES was too slow to allow for accurate estimates of ROI-HO efficiency.

Reconstructions of the second and third thickest fibers from the ACR mammography accreditation phantom are shown in figure 4. The trends in signal conspicuity appear to match well with the trends in ROI-HO efficiency. In particular, note the 90° rod is more conspicuous than the 0° rod at low regularization strengths even though it has a smaller diameter, in agreement with the ROI-HO results.

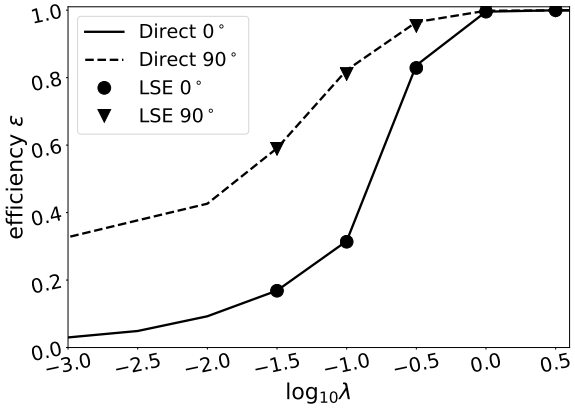

Figure 3. Comparison of ROI-HO efficiencies for detection of a rod of 0.75 mm width and 10.0 mm length oriented at 0° with respect to the x-axis and a rod of 0.61 mm width and 10.0 mm length oriented at 90°. Efficiencies were calculated using the direct and LSE methods with the 2D system model.

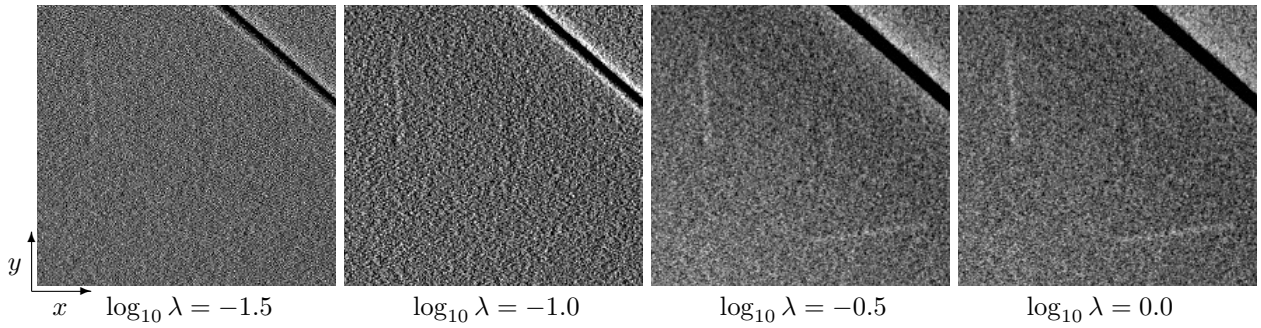

Figure 4. Real data PLS reconstructions of the rods of second (bottom right) and third (top left) largest diameter from the ACR mammography accreditation phantom at different regularization strengths. The lengths and diameters of the rods match those employed in calculating the ROI-HO efficiencies in Figure 3.

4. NEW WORK

Comparison of the ROI-HO as evaluated using the 2D and 3D system models for the rod signal and the LSE approach to calculating the ROI-HO are the new contributions of this work. The work has never been submitted for publication or presentation elsewhere.

5. CONCLUSIONS/DISCUSSION

The efficiency curves for the ROI-HO suggest that information relevant to task performance is better preserved with increasing regularization but also suggest a point at which increasing regularization yields diminishing returns. Agreement between the ROI-HO efficiencies calculated using the 2D and 3D system models suggests the possibility of performing reconstruction parameter optimization with the 2D model. This result is preliminary and further empirical studies are needed to determine whether the result still holds with larger 3D image volumes and different imaging tasks. For example, the extent to which the 2D model approximates the 3D model needs to be investigated for signals with varying x-z cross-sections as one would expect the approximation to be less accurate for such signals.

The transition region from low to high efficiency in the ROI-HO curves appears to be dependent on the orientation of the rod signal, with the rod oriented perpendicular to the x-axis exhibiting higher efficiencies at low regularization strengths. This orientation dependence was also seen to correspond with trends in conspicuity of ACR phantom reconstructions. As increasing regularization strength also comes at a cost to resolution, particularly in the z direction, further analysis of this orientation-dependence/resolution tradeoff needs to be performed.

The LSE approach to calculating the ROI-HO was effective over a wide range of regularization strengths and could potentially allow for calculation of ROI-HO efficiency for larger 3D volumes and tasks with more complex signal shapes and larger spatial extent. The current implementation of the approach fails at at small regularization strengths due to slow convergence rates, but the approach was able to cover a wide enough range of regularization strengths to identify much of the transition region between low and high efficiency for both orientations of the signal. Appropriate regularization of the equality constrained least squares problem in equation 2 may potentially allow for estimates at lower regularization strengths and is a subject for future work.

We note the correspondence between the 2D ROI-HO and results and the 3D ACR reconstructed images provide only preliminary indications. Many more empirical results are needed to establish a correspondence between the ROI-HO and signal detectability in real data reconstructions. Also, we note that we only discussed signal conspicuity with respect to the ACR phantom reconstructions, and detection efficiency and conspicuity, while related, are not equivalent.

ACKNOWLEDGMENTS

The authors would like to thank Drs. Adrian Sanchez, Chris Ruth, Yiheng Zheng, and Chao Huang for providing useful discussion. This work was supported in part by NIH R01 Grants Nos. CA182264, EB018102, and NIH F31 Grant No. EB023076. The contents of this article are solely the responsibility of the authors and do not necessarily represent the official views of the National Institutes of Health.

REFERENCES

[1] Sechopoulos, I., "A review of breast tomosynthesis. Part I. The image acquisition process," *Med. Phys.* **40**(39), 14301–5621 (2013).

[2] Maidment, A., "AAPM Medical Physics Tutorial Session 1: Digital Breast Tomosynthesis," Presented at the 2017 meeting of the Radiological Society of North America.

[3] Rose, S. D., Sanchez, A. A., Sidky, E. Y., and Pan, X., "Investigating simulation-based metrics for characterizing linear iterative reconstruction in digital breast tomosynthesis," *Med. Phys.* **44**(9), 279–296 (2017).

[4] Rose, S. D., Reiser, I., Sidky, E. Y., and Pan, X., "The non-prewhitening and Hotelling observers for parameter selection for linear iterative image reconstruction in breast tomosynthesis," in [*IEEE medical imaging and nuclear science symposium conference record*], (2017).

[5] Barrett, H. H. and Myers, K. J., [*Foundations of Image Science*], John Wiley & Sons, Hoboken, New Jersey (2004).

[6] Barlow, J. L., "Error analysis and implementation aspects of deferred correction for equality constrained least squares problems," *SIAM J. Numer. Anal.* **25**(6), 1340–1358 (1988).

[7] Choi, S.-C. T., Paige, C. C., and Saunders, M. A., "MINRES-QLP: A Krylov subspace method for indefinite or singular symmetric systems," *SIAM J. Sci. Comput.* **33**(4), 1810–1836 (2011).